

# Supporting Information for: CO oxidation by subnanometer $\text{Ag}_x\text{Au}_{3-x}$ supported clusters via DFT simulations

F. R. Negreiros,<sup>†</sup> L. Sementa,<sup>†</sup> G. Barcaro,<sup>†</sup> S. Vajda,<sup>‡</sup> E. Aprá,<sup>¶</sup> and A.  
Fortunelli<sup>\*,†</sup>

*CNR-IPCF, Istituto per i Processi Chimico-Fisici del Consiglio Nazionale delle Ricerche, Pisa,  
56124, Italy, Materials Science Division, Center for Nanoscale Materials, Argonne National  
Laboratory, Argonne, IL, 60439, USA & Department of Chemical and Environmental  
Engineering, Yale University, New Haven, CT, 06520, USA, and Computer Science and  
Mathematics Division, Oak Ridge National Laboratory, TN 37831, USA*

E-mail: alessandro.fortunelli@cnr.it

*Computational details* The search for the local minima configurations and for the transition states connecting them was performed starting from a large database of structures and saddle points previously generated via a Reactive Global Optimization approach.<sup>1</sup> Local minima from the structural database were used as initial configurations for re-optimizations, and saddle points for intrinsic reaction coordinate calculations.<sup>2</sup> Additional Basin-Hopping global optimization searches were also performed<sup>3,4</sup> with 300 Monte Carlo steps at a fictitious temperature of 500 K starting from each major configuration to enrich the previously obtained data set and increase the thoroughness

---

\*To whom correspondence should be addressed

<sup>†</sup>CNR-IPCF, Istituto per i Processi Chimico-Fisici del Consiglio Nazionale delle Ricerche, Pisa, 56124, Italy

<sup>‡</sup>Materials Science Division, Center for Nanoscale Materials, Argonne National Laboratory, Argonne, IL, 60439, USA & Department of Chemical and Environmental Engineering, Yale University, New Haven, CT, 06520, USA

<sup>¶</sup>Computer Science and Mathematics Division, Oak Ridge National Laboratory, TN 37831, USA

of the PES sampling. All the calculations were performed at the density-functional theory (DFT) level using the plane-wave Quantum Espresso package.<sup>5</sup> The Perdew-Burke-Ernzerhof (PBE)<sup>6</sup> exchange-correlation functional was used together with ultrasoft pseudopotentials<sup>7</sup> and energy cutoffs of 40 Ry and 320 Ry for the wave function and electronic density, respectively. Structural optimizations and transition state searches were carried out in a spin-unrestricted formalism, using 3x4 and 4x4 cells with 2 MgO layers (kept frozen during structural optimizations), 17 Å of empty space between replicated cells and a Brillouin zone sampled at the Gamma point only. In order to accurately describe transition state energetics, reaction barriers were evaluated with a nudged elastic band (NEB) transition state algorithm<sup>8</sup> using the Broyden scheme in a two-step approach: a first NEB on the full reaction-path using 8-10 intermediate images; a second NEB with initial and final states close to the transition state, using 4-8 intermediate images and the climbing-image procedure. In terms of accuracy, our theoretical approach somewhat overestimates the experimental value of the reaction energy for CO oxidation, predicting 6.53 eV vs 5.86 eV from experiment. We finally note that entropic factors to the reaction free energy were evaluated by neglecting vibrational contributions.

Charge density differences were performed using the QE package following the details given in the last paragraph. Mulliken charge analysis were performed using the NWChem<sup>9</sup> package version 5.1.1 and a cluster model consisting of a 3x3 cell plus an array of  $\pm 2.0$  au point charges (about 1500) extending for four layers in the direction perpendicular to the surface and up to  $\approx 10$  from the borders of the cluster in the (100) surface plane. The atoms of the central cluster and the point charges around it were located at the lattice positions of the MgO rock-salt bulk structure at the experimental lattice constant of 4.208. Gaussian-type orbital basis sets of double-z quality for all elements and 19-valence electron effective core potential for Ag and Au<sup>10</sup> were used.

In the following slide we report the adhesion energies of the pure metal clusters on MgO(001) and also of the catalytic species  $\text{Au}_3\text{CO}$ ,  $\text{Ag}_1\text{Au}_2\text{CO}$ ,  $\text{Ag}_2\text{Au}_1\text{CO}_3$  and  $\text{Ag}_3\text{CO}_3$ . Then, in the next 4 slides, we report some representative structures with the corresponding energetics of  $\text{M}_3$  (second slide),  $\text{M}_3\text{O}_2$  (third slide),  $\text{M}_3\text{O}_2\text{CO}$  (fourth slide) and  $\text{Ag}_3(\text{CO}_3)_2$  clusters supported on

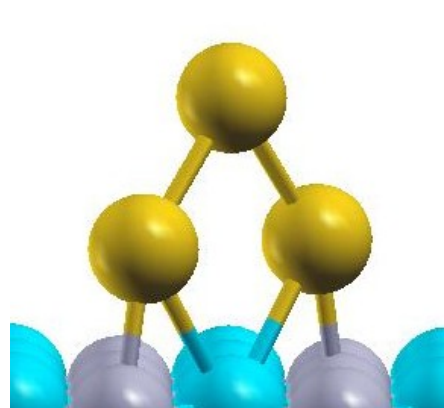
MgO(100) (fifth slide). In addition, in the sixth slide we show the spin density for six representative configurations,  $\text{Ag}_3$ ,  $\text{Ag}_3\text{O}_2$ ,  $\text{Ag}_3\text{CO}_3$ ,  $\text{Au}_3$ ,  $\text{Au}_3\text{O}_2$  and  $\text{Au}_3\text{CO}_3$ . Last, in the last three slides we report a charge analysis of the interaction of a carbonate species with  $\text{Ag}_3$  and  $\text{Au}_3$  clusters in the gas-phase, two  $\text{Ag}_2\text{Au}_1$  homotops supported on MgO(100) and a  $\text{Ag}_3$  cluster with the carbonate non-interacting and interacting with the MgO(100) surface.

## References

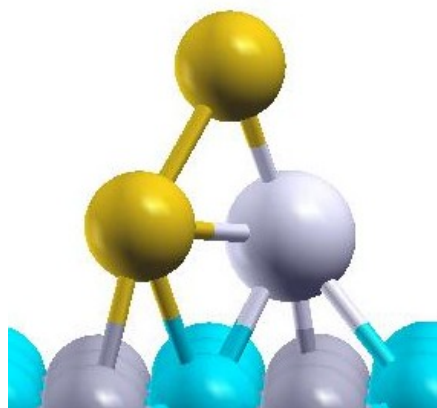
- (1) Negreiros, F. R.; Aprá, E.; Barcaro, G.; Sementa, L.; Vajda, S.; Fortunelli, A. *Nanoscale* **2012**, *4*, 1208.
- (2) Gonzalez, C.; Schlegel, H. *J. Chem. Phys.* **1989**, *90*, 2154.
- (3) Wales, D. J.; Scheraga, H. A. *Science* **1999**, *1368*, 285.
- (4) Barcaro, G.; Aprá, E.; Fortunelli, A. *Chem. Eur. J.* **2007**, *13*, 6408.
- (5) Giannozzi, P. et al. *J. Phy.: Condensed Matter* **2009**, *21*, 395502 (19pp).
- (6) Perdew, J.; Burke, K.; Ernzerhof, M. *Phys. Rev. Lett.* **1996**, *77*, 3865.
- (7) Vanderbilt, D. *Phys. Rev. B* **1990**, *41*, 7092.
- (8) Henkelman, G.; Uberuaga, B. P.; Jonsson, H. *J. Chem. Phys.* **2000**, *113*, 9901.
- (9) Bylaska, E. J. et al. NWChem, A Computational Chemistry Package for Parallel Computers, Version 5.0, Pacific Northwest National Laboratory, Richland, Washington 99352-0999, USA. 2006.
- (10) Andrae, D.; Haeussermann, U.; Dolg, M.; Stoll, H.; Preuss, H. *J. A. Chem. So.* **1990**, *77*, 123.



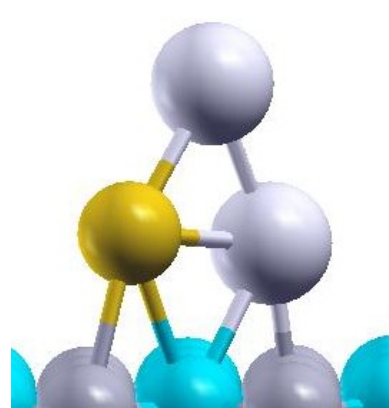
## Adhesion energies on MgO(001)



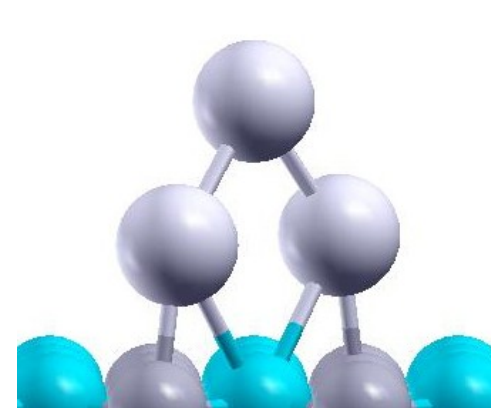
*1.58eV*



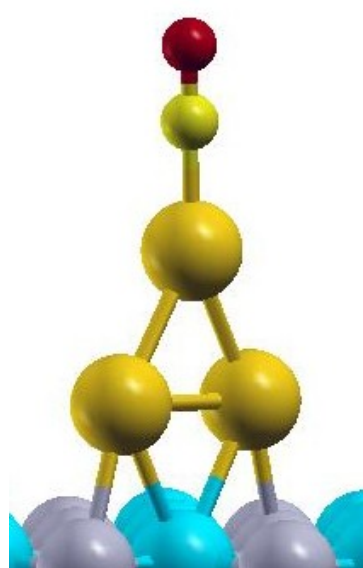
*1.07eV*



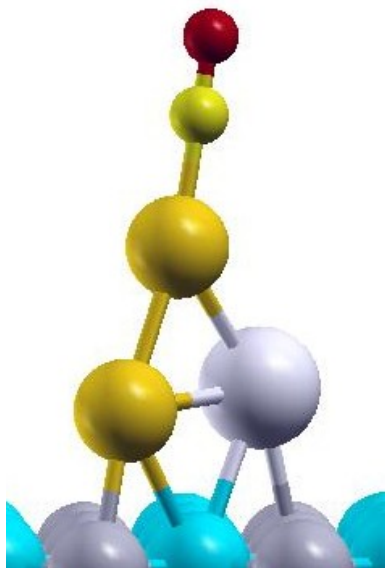
*0.92eV*



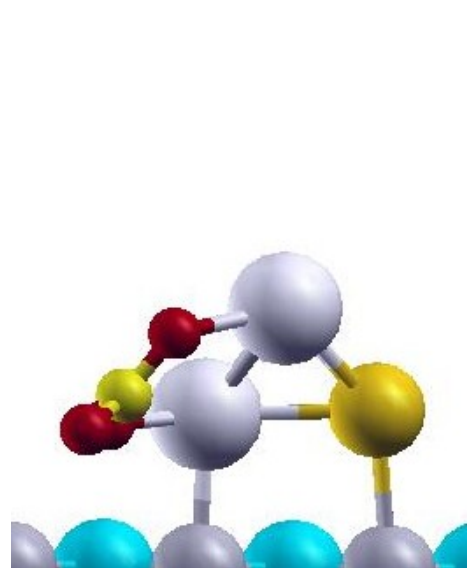
*0.91eV*



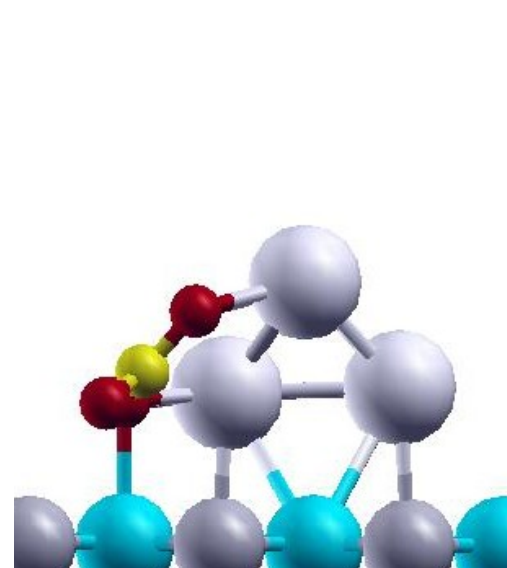
*1.08eV*



*1.04eV*


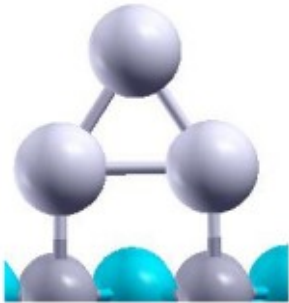




*1.20eV*

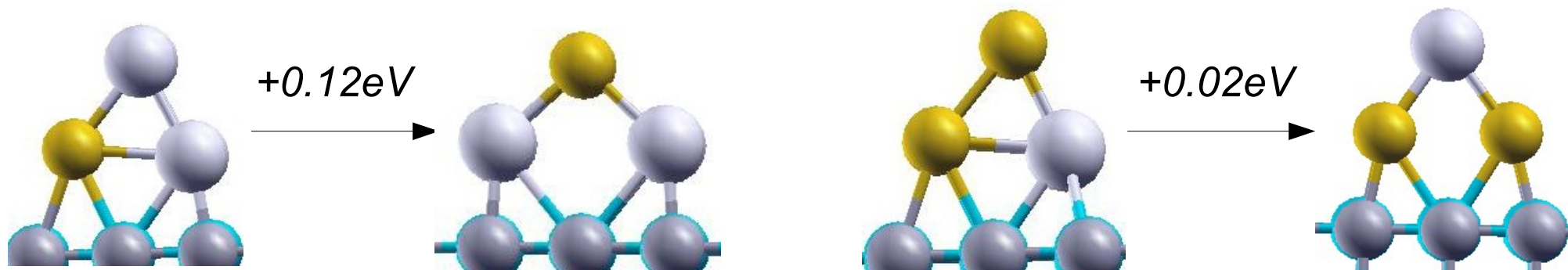


*1.25eV*

# Relative energies: bare metal clusters – $M_3/\text{MgO}(001)$

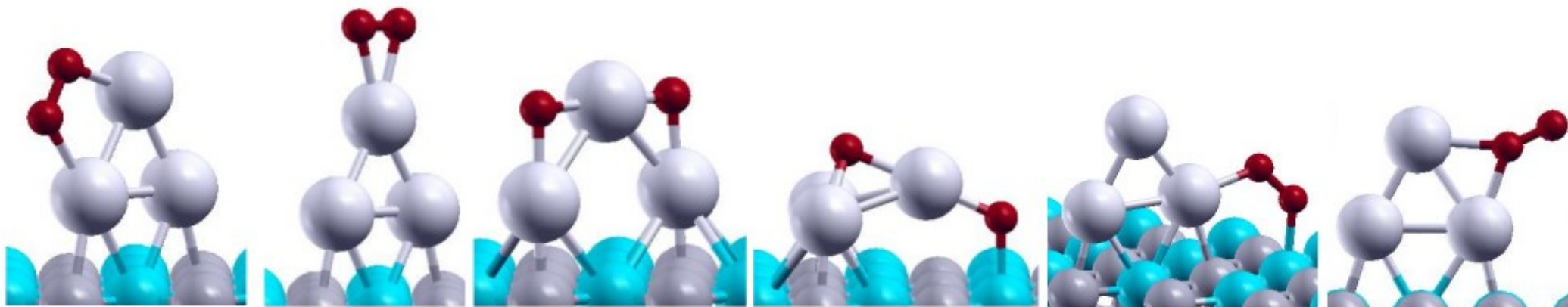
				
$\text{Au}_3$	0.00	+0.19	+0.13	–
$\text{Ag}_1\text{Au}_2$	0.00	0.00	+0.14	+0.48
$\text{Ag}_2\text{Au}_1$	0.00	0.00	+0.22	+0.12
$\text{Ag}_3$	0.00	+0.06	+0.19	+0.20

homotop energetics for alloys



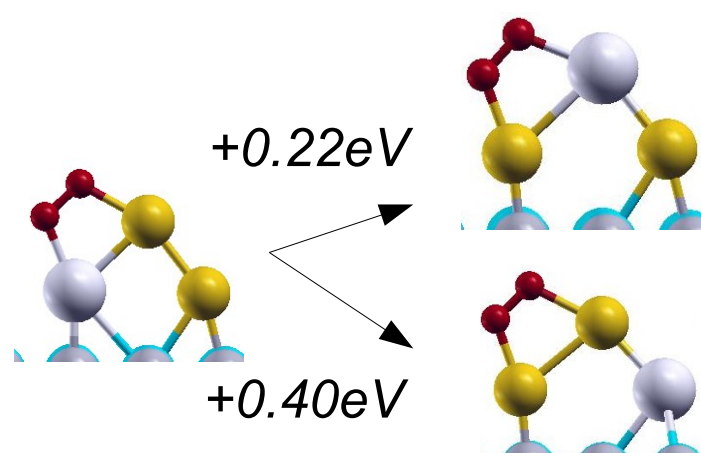
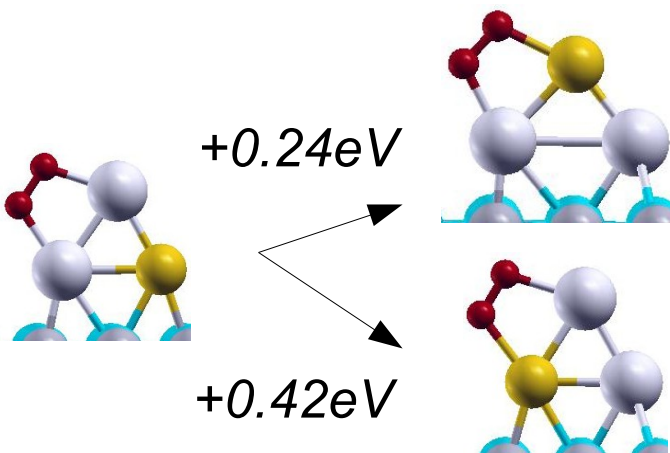


Relative energies:  $M_3O_2/MgO(001)$

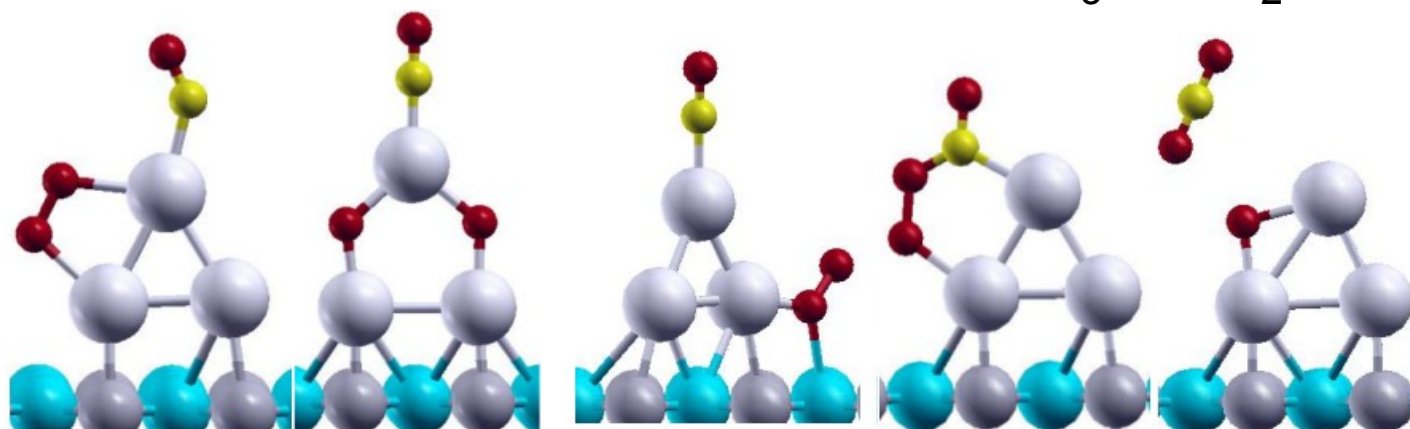


0.00	+0.09	-1.26	+0.33	+0.22	+0.56
0.00	+0.19	-0.93	-0.18	+0.18	-
0.00	+0.21	-0.56	-0.33	+0.12	-
0.00	+0.17	-0.46	+0.13	-0.01	+0.46

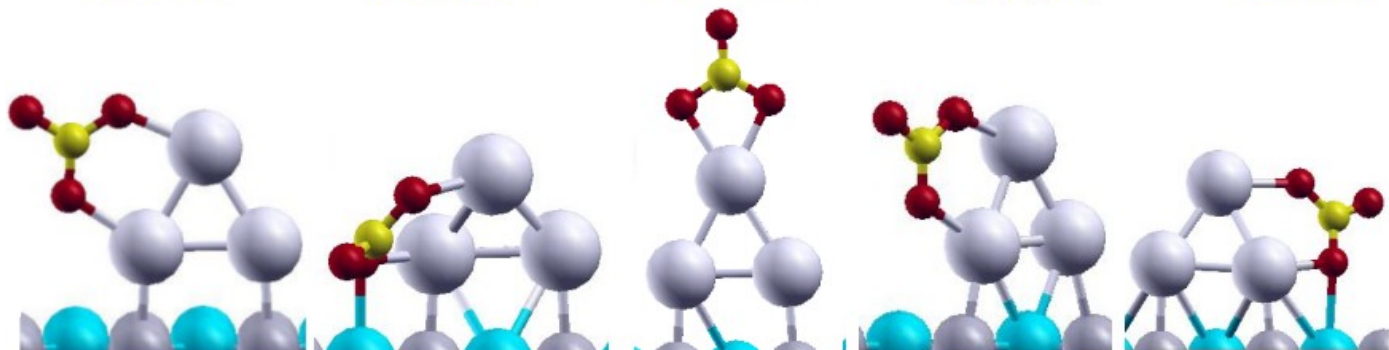
homotop energetics for alloys



# Relative energies: $M_3\text{COO}_2/\text{MgO}(001)$

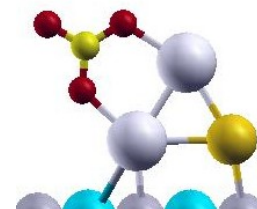


0.00	-0.77	-0.20	+0.11	-2.06
0.00	-0.43	-0.13	+0.11	-1.92
0.00	-0.37	+0.03	+0.08	-2.25
0.00	-0.25	-0.02	-0.04	-2.35

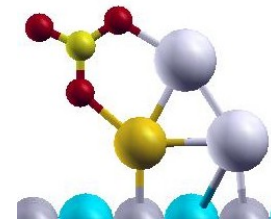
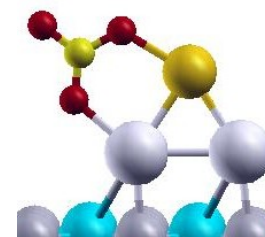


-2.63	-2.36	-2.60	-2.59	-2.57
-2.89	x	-2.59	x	x
-3.35	-3.44	-2.92	-3.32	-3.23
-3.41	-3.66	-3.15	-3.41	-3.42

homotop energetics  
for alloys

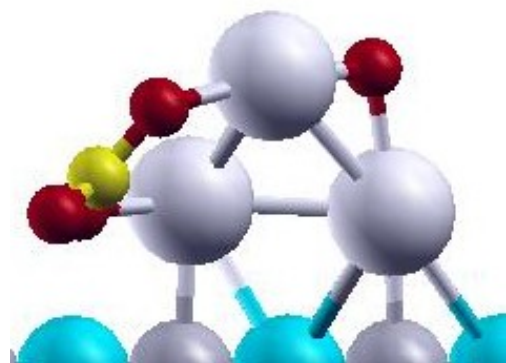


+0.35eV      +0.58eV



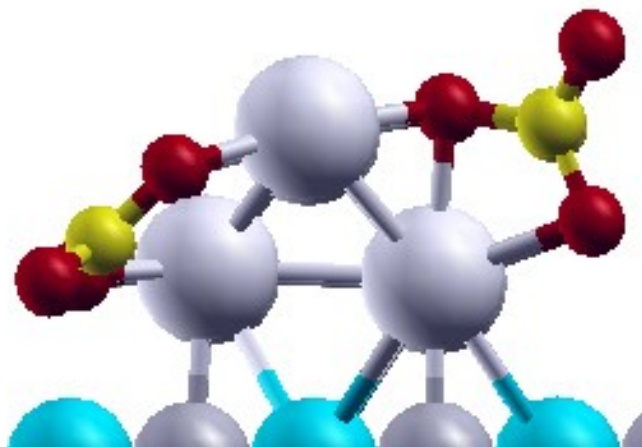


Relative energies:  $\text{Ag}_3(\text{CO})_2\text{O}_2$  and  $\text{Ag}_2\text{Au}_1(\text{CO})_2\text{O}_2$



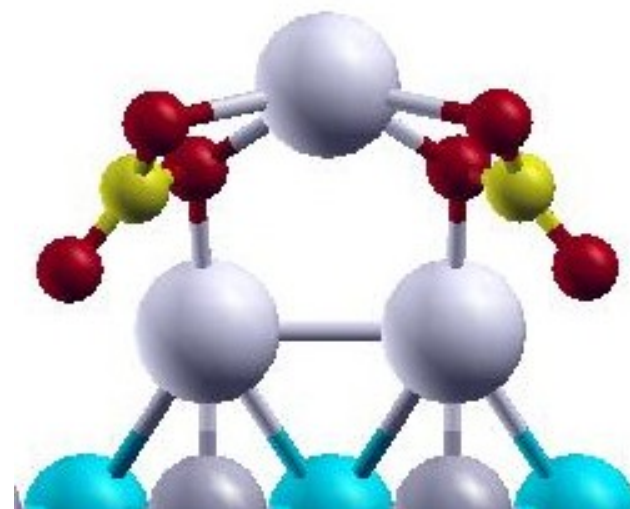
$0.00\text{eV}$

$0.00\text{eV}$



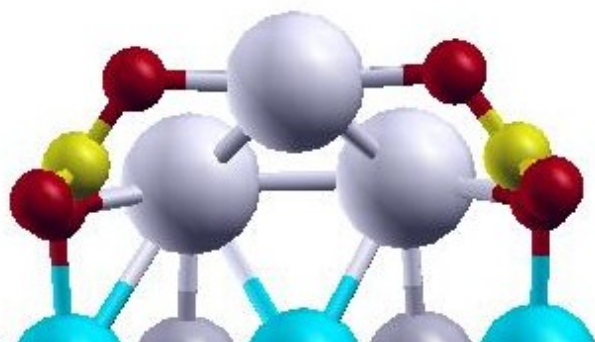
$+0.07\text{eV}$

$-0.36\text{eV}$



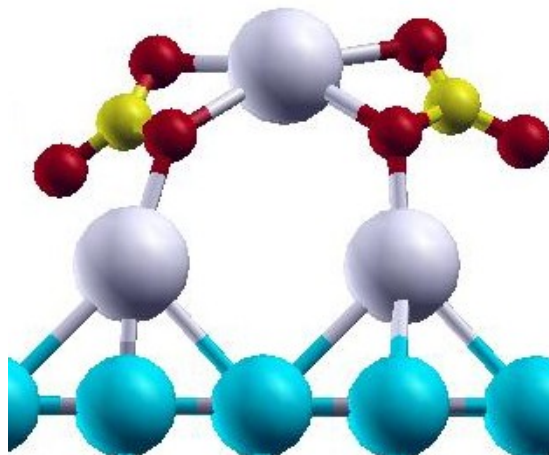
$-0.01\text{eV}$

$-0.41\text{eV}$



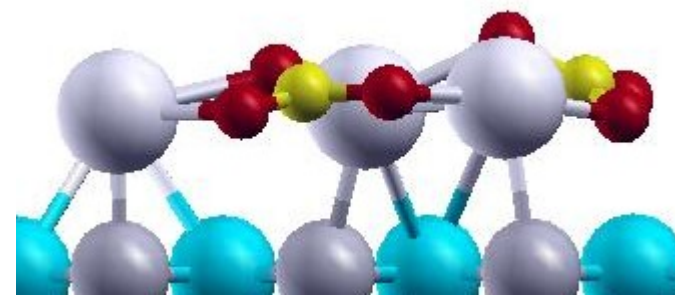
$+0.64\text{eV}$

$-0.21\text{eV}$



$-0.20\text{eV}$

$-0.51\text{eV}$

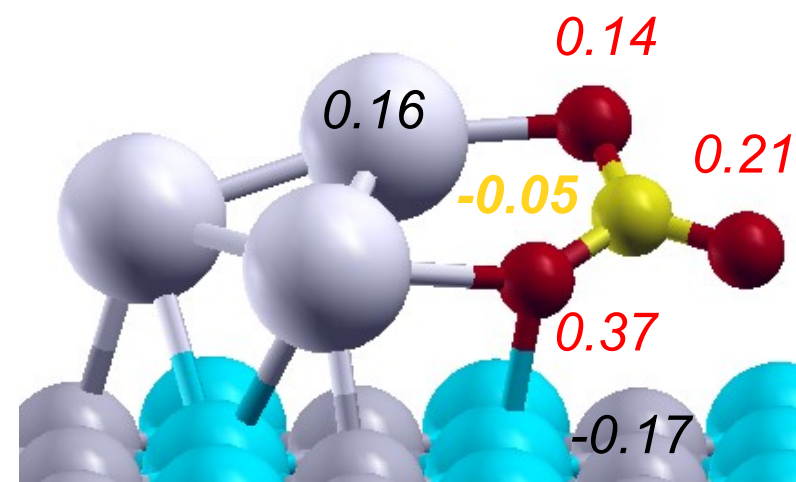
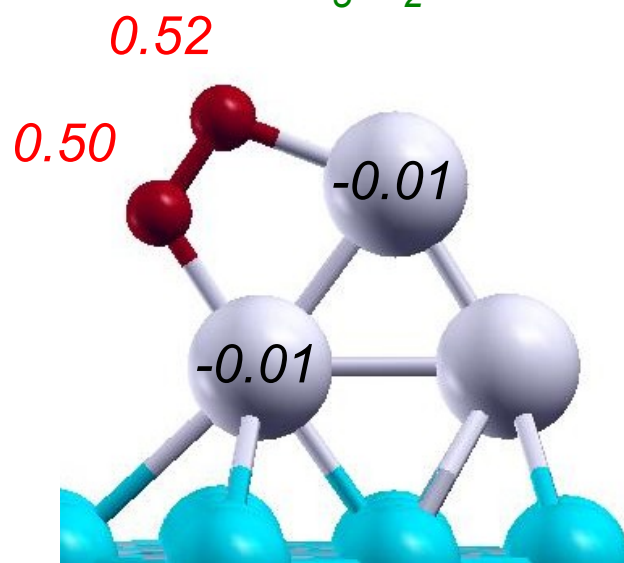
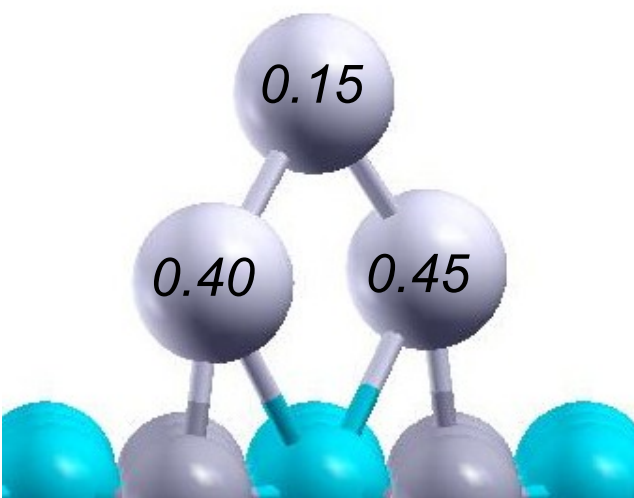
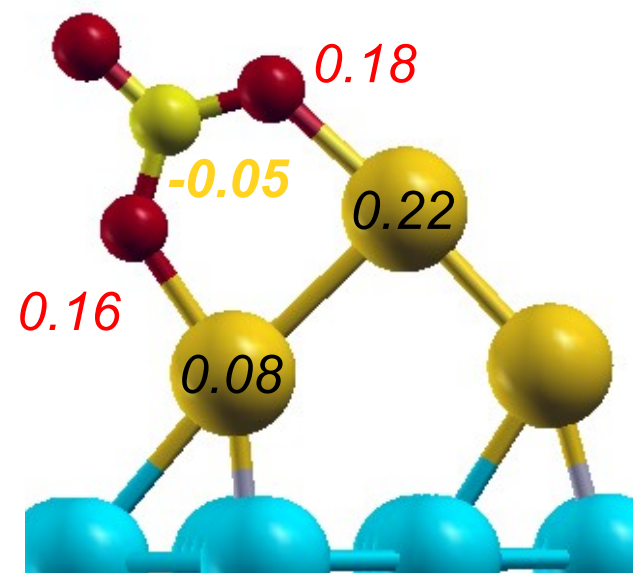
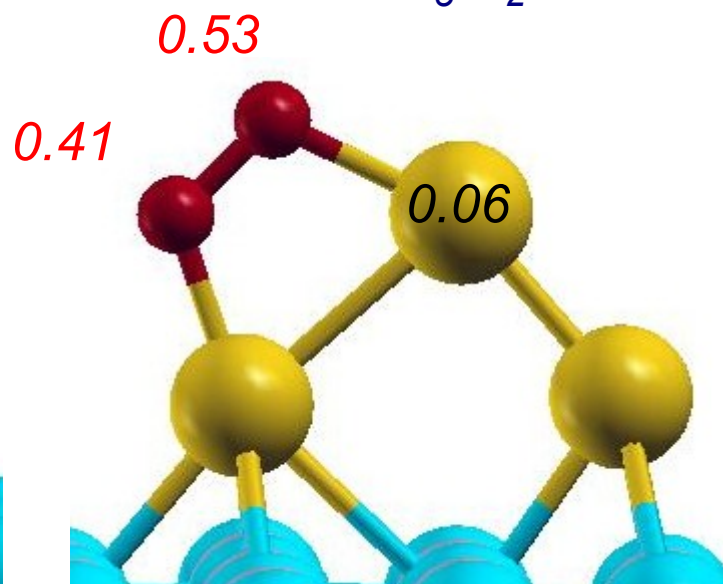
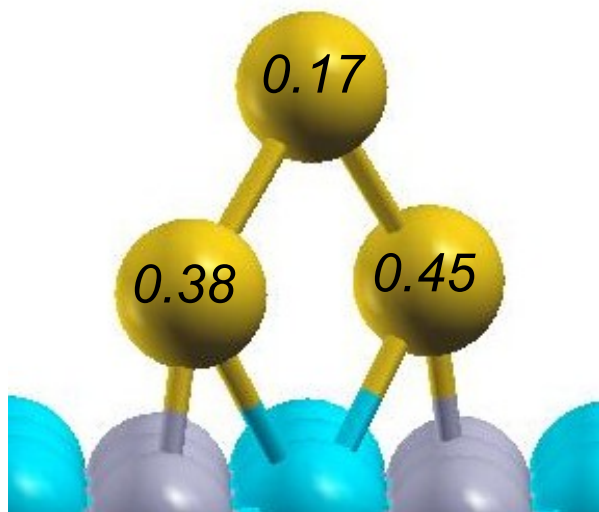


$-0.60\text{eV}$

$-1.03\text{eV}$

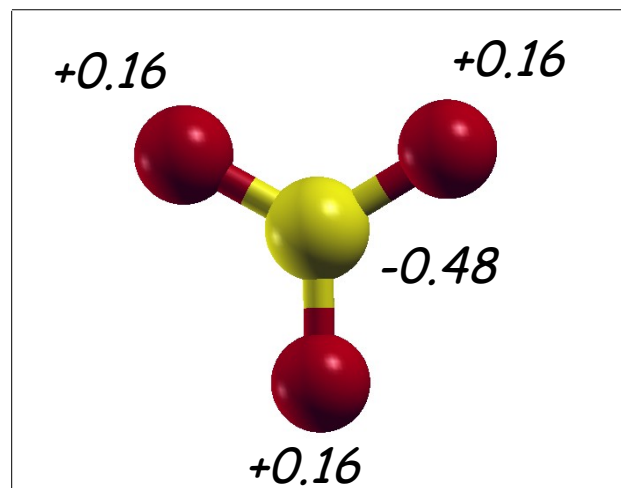


# Spin density – Mulliken analysis (NWChem)

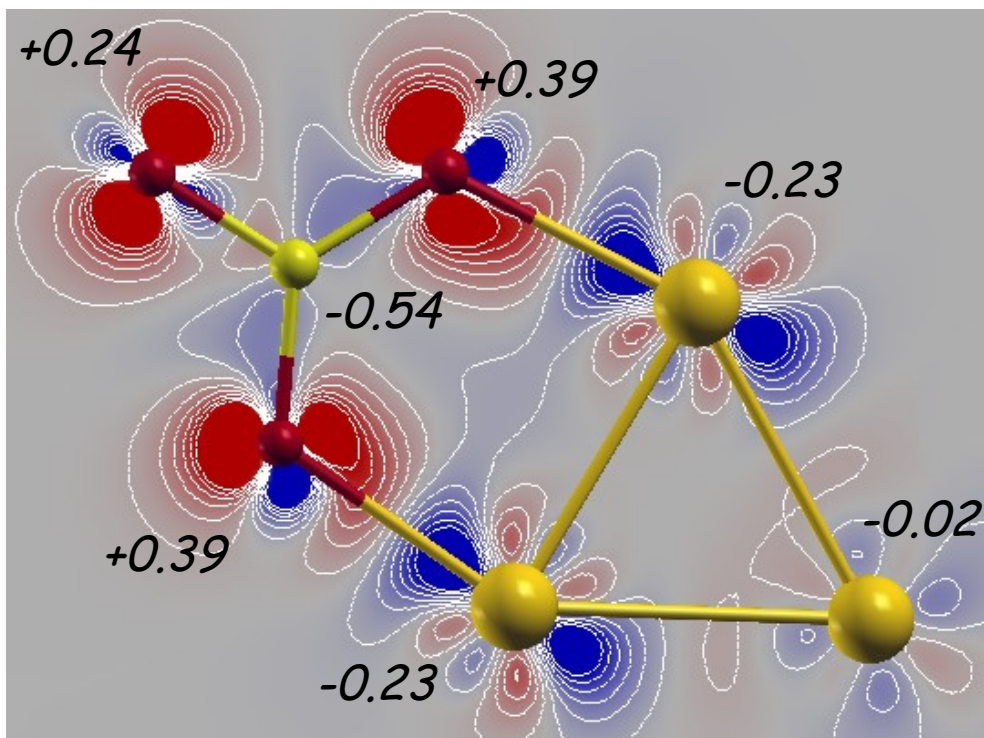


*The magnetic moment is equal to  $1\mu_B$  (one electron unpaired) in all cases*

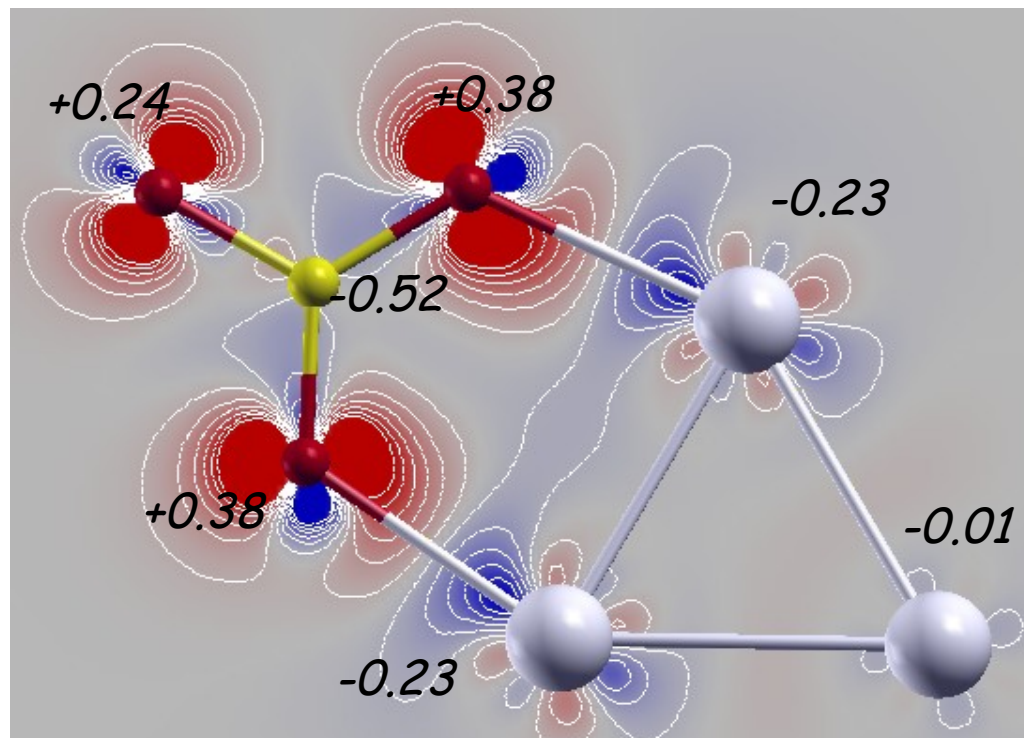
# gas-phase $M_3CO_3$ : Mulliken and charge density difference



$Au_3$



$Ag_3$

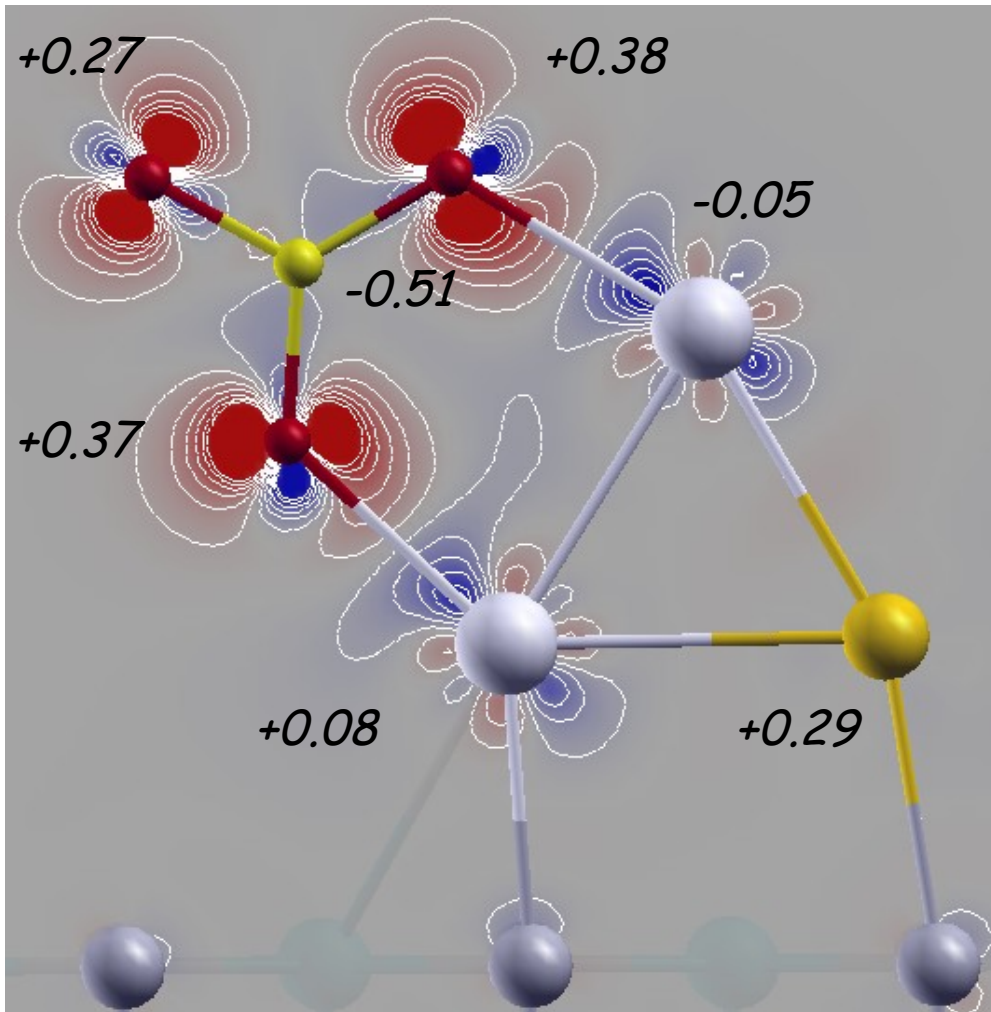


larger charge gain for the oxygen atoms in contact with the metal atoms  
no real differences between  $Ag_3$  and  $Au_3$ : the charge transfer is about the same

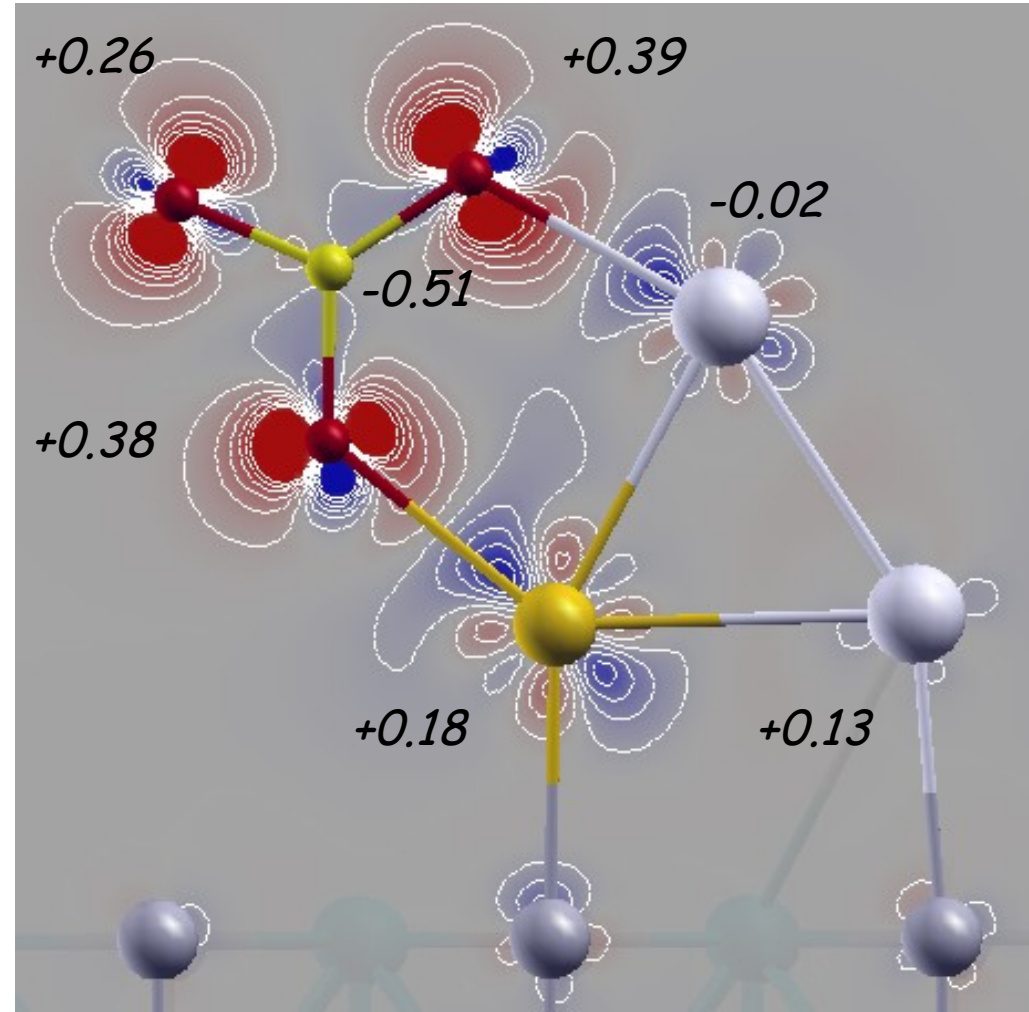
Values in black are the charge variation (Mulliken-NWChem)



$$\text{Ag}_2\text{Au}_1\text{CO}_3: \Delta\rho = \rho(\text{Ag}_2\text{Au}_1\text{CO}_3\text{MgO}) - \rho(\text{Ag}_2\text{Au}_1\text{MgO}) - \rho(\text{CO}_3)$$



*charge loss from the surface:  $0.83e^-$*

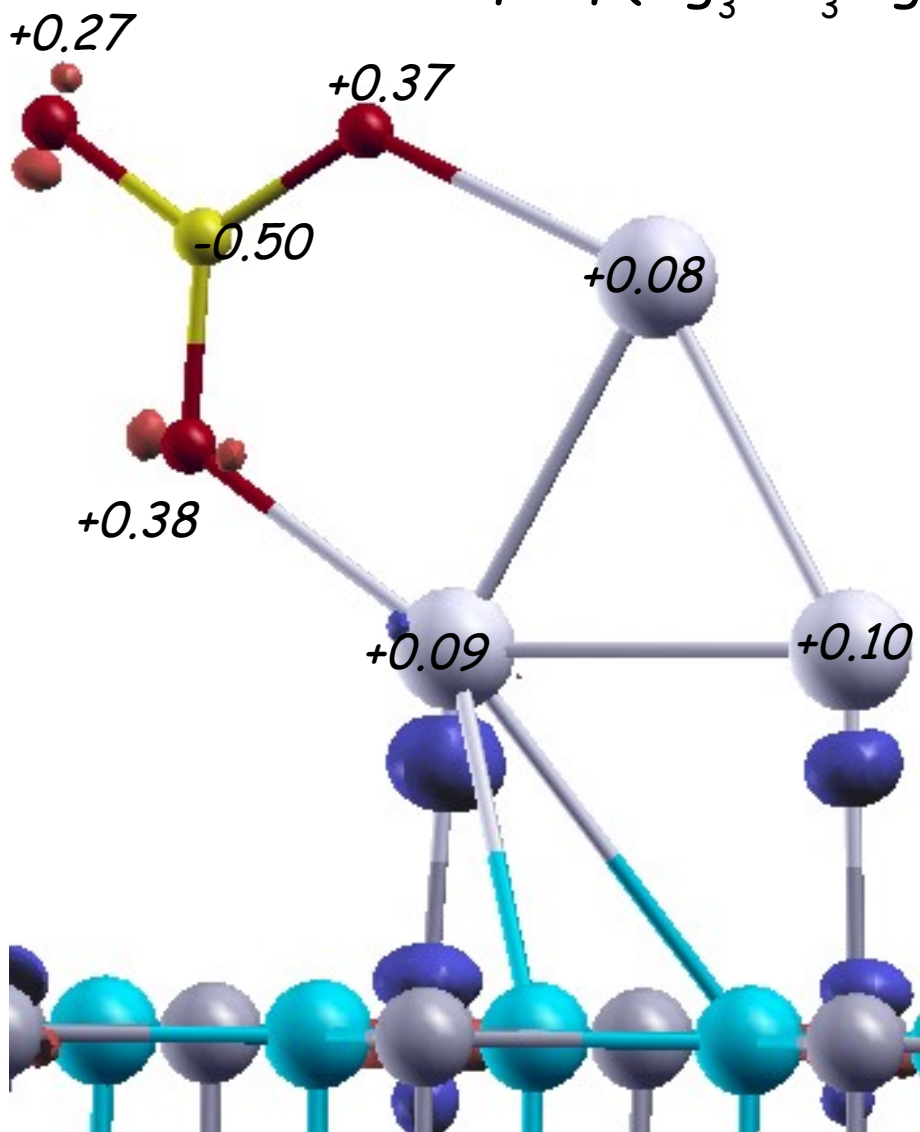


*charge loss from the surface:  $0.83e^-$*

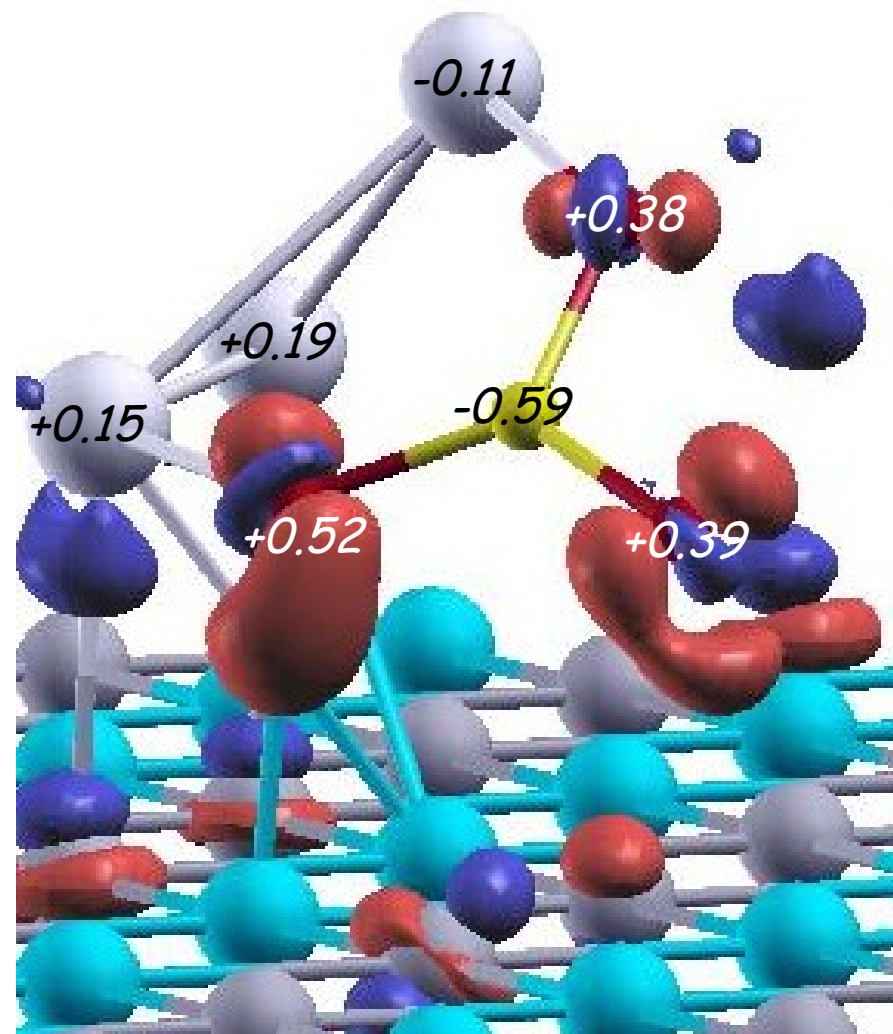
*no additional charge transfer from the metal to the carbonate after it is supported, only from the surface to the metal cluster*  
*the carbonate is less stable when formed on the Au-side by  $\approx 0.6\text{eV}$*

$\text{Ag}_3\text{CO}_3 \rightarrow \text{laid-down vs straight}$

$$\Delta\rho = \rho(\text{Ag}_3\text{CO}_3\text{MgO}) - \rho(\text{Ag}_3\text{CO}_3) - \rho(\text{MgO})$$



charge loss from the surface:  $0.79e^-$



charge loss from the surface:  $0.93e^-$

carbonate interaction with the surface is energetically favorable for  $\text{Ag}_3$ , not  $\text{Au}_3$ , and entails a larger charge transfer from the surface to the carbonate